Numerical solution of the Navier-Stokes equations for hypersonic ramps with the NS3GR solver

François Dubois, Olivier Michaux

Workshop on Hypersonic Flows for Reentry Problems,
Part II, Antibes (France), april 15-19, 1991. May 1992

Numerical Solution of the Navier-Stokes Equations for Hypersonic Ramps with the NS3GR Solver.

François DUBOIS and Olivier MICHAUX
Aerospatiale, Space & Defense, Department of Applied Mathematics
and Scientific Computing, BP 96, F-78133 Les Mureaux Cedex, France.

Abstract.

Test cases III.1, III.2, III.4 have been solved with a preliminary version of the computer code NS3GR developed at Aerospatiale Les Mureaux. We describe the present version of the computer code (Section 1), the generation of the mesh (Section 2) and the numerical results (Section 3).

I. Description of the Navier-Stokes Solver NS3GR.

The computer code NS3GR (Navier Stokes Non Structuré Tridimensionnel incluant des effets de Gaz Réel) is under study at the Technical Direction of the Space and Strategic Systems Division of Aerospatiale since 1988. It is an extension of the Euler solver CEL3GR presented at the previous INRIA-GAMNI-SMAI hypersonic workshop in 1990 (Dubois-Michaux [1992]). It is based on the finite volume MUSCL scheme (Van Leer [1979]) and the use of finite element type unstructured meshes. In the present version only the particular case of a polytropic perfect gas on two-dimensional geometries with structured meshes is studied.

This contribution has been published in *Hypersonic Flows for Reentry Problems, Volume 3, Proceedings of the INRIA-GAMNI/SMAI Workshop on Hypersonic Flows for Reentry Problems, Part II, Antibes, France, 15–19 April 1991*, Editors Rémi Abgrall, Jean-Antoine Désidéri, Roland Glowinski, Michel Mallet, Jacques Périaux, Springer Verlag, pages 258-269, 1993. Edition January 2024.

Workshop on Hypersonic Flows for Reentry Problems,
Part II, Antibes (France), april 15-19, 1991. May 1992

Numerical Solution of the Navier-Stokes Equations for Hypersonic Ramps with the NS3GR Solver.

François DUBOIS and Olivier MICHAUX
Aerospatiale, Space & Defense, Department of Applied Mathematics
and Scientific Computing, BP 96, F-78133 Les Mureaux Cedex, France.

Abstract.

Test cases III.1, III.2, III.4 have been solved with a preliminary version of the computer code NS3GR developed at Aerospatiale Les Mureaux. We describe the present version of the computer code (Section 1), the generation of the mesh (Section 2) and the numerical results (Section 3).

I. Description of the Navier-Stokes Solver NS3GR.

The computer code NS3GR (Navier Stokes Non Structuré Tridimensionnel incluant des effets de Gaz Réel) is under study at the Technical Direction of the Space and Strategic Systems Division of Aerospatiale since 1988. It is an extension of the Euler solver CEL3GR presented at the previous INRIA-GAMNI-SMAI hypersonic workshop in 1990 (Dubois-Michaux [1992]). It is based on the finite volume MUSCL scheme (Van Leer [1979]) and the use of finite element type unstructured meshes. In the present version only the particular case of a polytropic perfect gas on two-dimensional geometries with structured meshes is studied.

The conservation laws of mass, momentum and energy are integrated in space in each finite volume denoted by K. In this way a system of ordinary differential equations for the mean values of the conservative variables U_K is derived :

$$(1) \qquad |K| \frac{dU_K}{dt} + \sum_{f \in \partial K} |f| \left(\Phi^E(f) + \Phi^V(f) \right) = 0$$

where ∂K denotes the boundary of K, f a generic face of ∂K and $|f|$ (respectively $|K|$) its surface (respectively the volume of the cell K). The Euler flux $\phi^E(f)$ is computed according to the **second order accurate in space** MUSCL approach. We refer to Dubois-Michaux [1992] for a precise description of this numerical scheme. We focus here on the fact that in the CEL3GR / NS3GR code numerical scheme for the computation of gradients and slope limitation steps are truly multidimensional ; the step of approximating the solution of a 1D Riemann

problem remains the only monodimensional step : the waves issued from the corners and the edges of ∂K are neglected and only the waves generated by the two-dimensional interfaces are taken into consideration for the upwinding associated with the numerical scheme. For a precise treatment of contact discontinuities we have replaced the Sanders-Prendergast flux splitting by the approximate Riemann solver proposed by Osher [1981].

For a Newtonian fluid satisfying the Stokes hypothesis, the viscous flux $\phi^V(f)$ has a classical expression which is not detailed here (see e.g. Landau-Lifchitz [1953]). We remark that $\phi^V(f)$ is a simple algebraic function of the mean values and the gradients of velocity $\mathbf{u}$ and temperature T on the face f. We detail in the following the choices that have been done for computing the gradient of a typical scalar field. We remark simply that derivation is a **linear** and **local** operator. Therefore in NS3GR computer code the numerical approximation of the gradient of, saying, temperature on the face f, is supposed to be a linear functional of the degrees of freedom $\sigma(T)$ lying in the vicinity $V(f)$ of this face :

$$\nabla T\,(f) = \sum_{\sigma \in V(f)} \alpha(f,\sigma)\ \sigma(T)\ . \tag{2}$$

Assuming that even though our code is three-dimensional, for the sake of simplicity, we shall describe our method in the two-dimensional case with a structured mesh. In this case, the family $V(f)$ is composed by the six elements lying on each side and on the top and bottom of the face f. The coefficients $\alpha(f,\sigma)$ coupling the face f and the six elements of $V(f)$ are evaluated as follows : the relation (2) is supposed to be **exact** for temperature fields $T(\mathbf{x})$ lying in the six-dimensional linear space $LS(f)$

$$LS(f) = P_1(\mathbf{n}(f)) \otimes P_2(\tau(f)) \tag{3}$$

where $P_1(\mathbf{n}(f))$ (respectively $P_2(\tau(f))$) is the set of polynomials of degree 1 (respectively degree 2) relatively to the normal component $\mathbf{x}\bullet\mathbf{n}(f)$ (respectively $\mathbf{x}\bullet\tau(f)$) of point $\mathbf{x}$. In the particular case of a uniform mesh, we recover the classical finite-difference centered scheme (derived e.g. in Hollanders-Lerat-Peyret [1985]) :

$$\nabla T_{i+1/2,\,j} = \frac{1}{\Delta x}\left(T_{i+1,\,j} - T_{i,\,j}\right)\ \mathbf{n}(f) + \frac{1}{4\Delta y}\left(T_{i,\,j+1} + T_{i+1,\,j+1} - T_{i,\,j-1} - T_{i+1,\,j-1}\right)\ \tau(f). \tag{4}$$

For boundary faces, the vicinity V(f) consits of 9 degrees of freedom to assure consistency for regular meshes, as detailed in Dubois [1992]. These degrees of freedom are associated with cell centers as previously or with degrees of freedom on boundary faces to take into account the boundary condition : Dirichlet for a rigid wall or homogeneous Neumann for a symmetry plane.

The differential system (1) is integrated in time with a **second order accurate explicit** scheme of Heun (Runge-Kutta of order 2). The present Navier Stokes version of the code NS3GR has been developed in 1990 on the Cray XMP of Aerospatiale Les Mureaux.

II. Description of the Mesh Generation.

The quality of a Navier-Stokes numerical solution is strongly affected both by the numerical scheme and the choice of the mesh. Note that we easily solve this 2-D problem with our 3-D solver by introducing two walls in the third direction, and just one cell between the two walls. We describe in this part the so-called fine mesh that has been chosen for test case III.2. Along the flat plate of lengh L = 0.126 a total number of 91 faces are equally distributed. Moreover, 8 extra faces are added for $-0.0111 \leq x \leq 0$ in front of the flat plate in order to capture the shock wave induced by the leading edge of the plate ; for those faces a boundary condition of symmetry is used. Along the ramp region ($0.126 \leq x \leq 0.197$) 56 faces are equally distributed and followed by 20 extra faces (for $0.197 \leq x \leq 0.223$) in order to minimize the error induced in the subsonic boundary layer by the outflow numerical boundary conditions (homogeneous Neumann for both velocity and temperature). We have used a Dirichlet boundary condition for velocity ($\mathbf{u} = 0$) and temperature (T = 290 K) for all the 175 faces along the plate, the ramp and the added faces. In this way we construct 175 vertices along the flow direction. The mesh consists of straight lines parallel to the y-direction issued from these 176 vertices. At the inflow ($x = -0.0109$) a constant value of $\Delta y = 1.35\ 10^{-4}$ is used and 66 grid points are generated for $0 \leq y \leq 8.8\ 10^{-3}$. The external boundary is a straight line with an angle $\alpha = 10\ °$ relatively to the x-axis. For each column $x = x_j$ of vertices the first mesh point inside the domain satisfies $y_2 - y_1 = 1.35\ 10^{-4}$ and the other mesh points are generated in order to obtain a geometric sequence whose ratio is evaluated with a Newton's algorithm.The aspect ratio for the cells along the flat plate is constant and we have $\Delta x / \Delta y = 10$. The fine mesh contains a total of 176 x 66 vertices and 11 375 control volumes ans is represented on Figure 1. A

coarse mesh with 84 x 30 vertices (4 faces before the plate, 46 along the plate, 30 along the ramp and 4 in the continuation of the ramp) has also been generated in order to obtain preliminary results on the plate and for the entire configuration.

For problem III.4, the same type of strategy for mesh generation have been used. The fine mesh contains 20 cells before the beginning of the plate, 114 on the plate (of lengh L = 0.442), 60 on the ramp (of lengh 0.2692) and 15 in the prolongation of the ramp. In the y direction, 65 cells are equally spaced for x = 0 ($\Delta y = 8.3\ 10^{-5}$) and form a geometric sequence for the other abscissae. The mesh contains a total of 13 585 elements (210 x 66 vertices). A coarse mesh containing only 117 x 30 vertices has been first used in order to compute a preliminary numerical solution.

III Presentation of the results.

The first case is problem **III.1**. The upstream Mach number is 10, the Reynolds number 143 800 per meter, the temperature at infinity 52 K, the wall temperature is 290 K and the ramp angle $\beta = 15°$. According to the requirements of Desideri-Periaux [1990], a modified Sutherland's law is used for the definition of viscosity $\mu(T)$ and a constant Prandtl number (Pr = 0.72) is assumed for the thermal conductivity coefficient. In this case, no recirculating zone appears (Figure 2) and our results are as well converged relatively to the mesh parameter.

The second test case (problem **III.2**) is analogous to the previous one except that the value of the ramp angle is now $\beta = 20°$. A recirculating bubble is observed (Figure 3). We have compared on Figures 4 and 5 the wall values of Cp coefficient and Stanton number for both problems III.1 and III.2. The recirculating zone appears clearly for problem III.2 on the Cf distribution (Figure 6) and is located for abscissae satisfying $0.116 \leq x \leq 0.156$. We observe also a small overshoot in the Cf curve, correlated to the corner point at x = 0.126.

Our third test case is problem **III.4**. It corresponds to experiments presented by Holden [1978]. The viscosity law and Prandtl number are analogous to the previous test cases. The upstream Mach number and Reynolds number per meter are equal to 11.68 and 558 000 respectively, the temperatures at infinity and on the body are respectively equal to 64.4 and 297.2 Kelvins. The angle of the ramp is only $\beta = 15°$. The iso-value contours of density ρ / ρ_∞ are presented on Figure 7.

The wall values of Cp coefficient, Stanton number Ch and skin friction Cf are displayed on Figures 10, 11, 12. We observe a good prediction of the recirculating zone on two different meshes (cf curve on Figure 12) in agreement with Holden's data.

Conclusion.

In the test cases on two-dimensional ramp flows the computer code NS3GR developed at Aerospatiale DSSS (Les Mureaux) has proved its capability to solve the Navier Stokes equations of gas dynamics in hypersonic situations. Extensions to unstructured meshes in three-dimensional geometries and the modelization of real gas effects are under study.

Acknowledgments.

We thank Antoine Joulot for helpful comments and stimulating discussions.

References.

Desideri J.A., Periaux J., Output Formats for Presentation of Computational Results, INRIA Sophia Antipolis, November 1990.

Dubois F. Interpolation de Lagrange et volumes finis. Une technique nouvelle pour calculer le gradient d'une fonction sur les faces d'un maillage non structuré, Aerospatiale Internal Report , ST/S n° 104 109, 1992.

Dubois F., Michaux O., Solution of the Euler Equations Around a Double Ellipsoidal Shape Using Unstructured Meshes and Including Real Gas Effects, Workshop on Hypersonic Flows for Reentry Problems, (Désidéri-Glowinski-Périaux Editors), Springer Verlag, vol 2, pp. 358-373, 1992.

Holden M.S., A Study of Flow Separation in Regions of Shock Wave-Boundary Layer Interaction in Hypersonic Flow, AIAA Paper 78-1169, 1978.

Hollanders H., Lerat A., Peyret R. Three Dimensional Calculation of Transonic Viscous Flows by an Implicit Method, AIAA J., **23**, pp. 1670-1678, 1985.

Landau L, Lifchitz E., **Fluid Mechanics**, Moscow 1953.

Osher S., Numerical Solution of Singular Perturbation Problems and Hyperbolic Systems of Conservation Laws, in **Mathematical Studies n° 47**, pp. 179-205, North Holland, Amsterdam, 1981.

Van Leer B., Towards the Ultimate Conservative Scheme V. A Second Order Sequel to Godunov's Method, J. Comp. Phys., **32**, pp. 101-136, 1979.

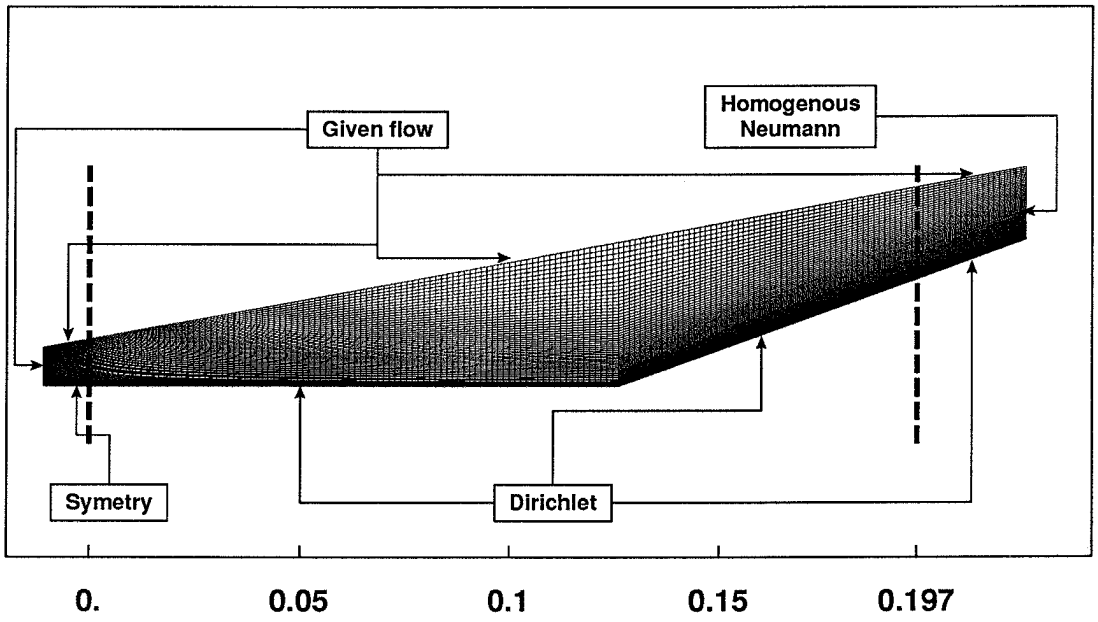

Figure 1. General view of the mesh for hypersonic ramps. (Problem III.2)

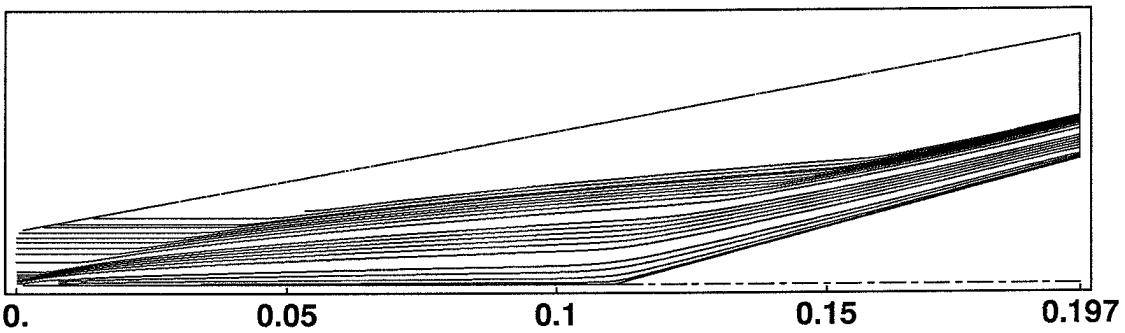

Figure 2. Problem III.1 (Mach = 10, Re = 143 000/m, beta = 15).
Streamlines.

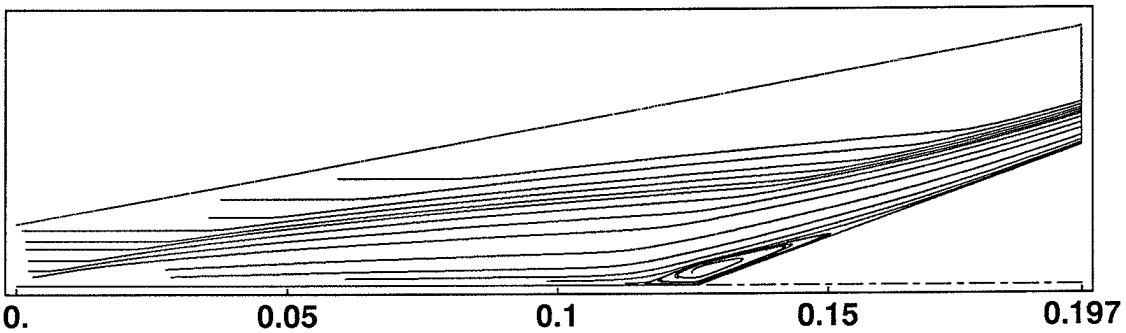

Figure 3. Problem III.2 (Mach = 10, Re = 143 000/m, beta = 20).
Streamlines.

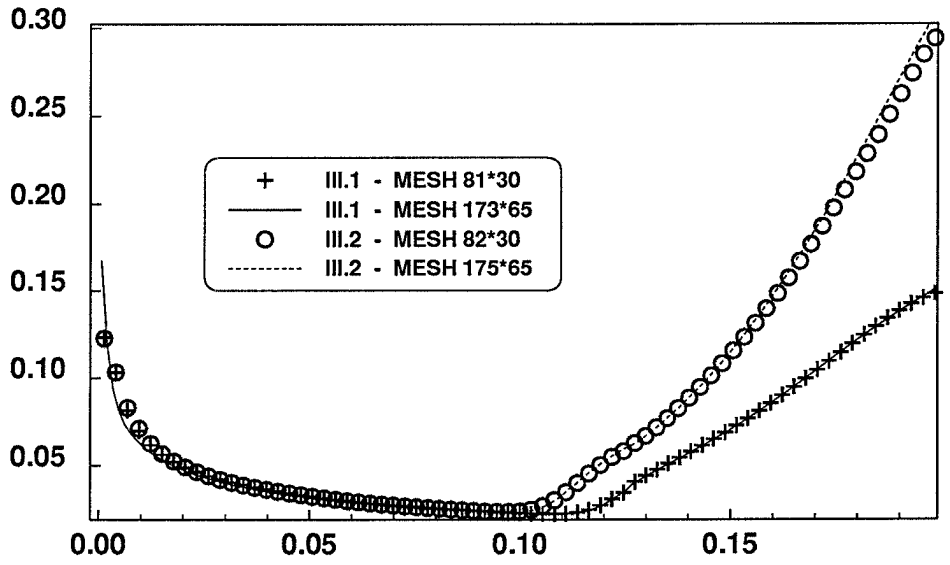

Figure 4. Problems III.1 and III.2. Pressure coefficient Cp.

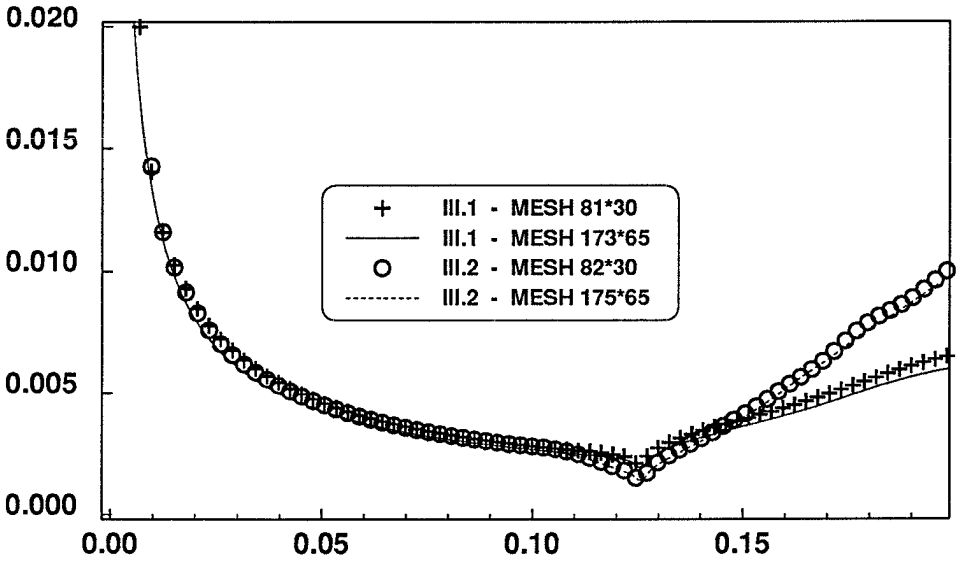

Figure 5. Problems III.1 and III.2. Stanton coefficient St.

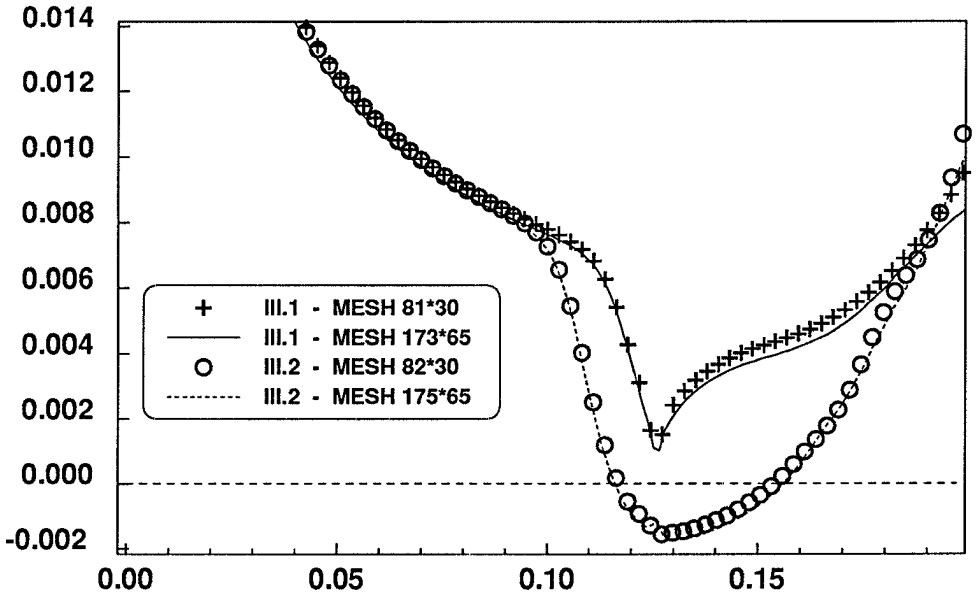

Figure 6. Problems III.1 and III.2. Skin friction coefficient Cf.

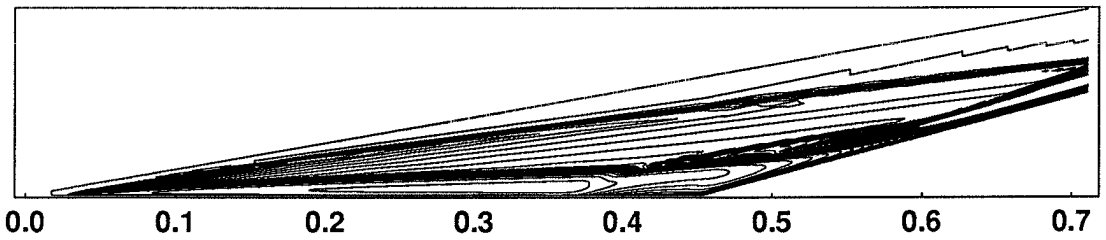

Figure 7. Problem III.4 (Mach = 11.68, Re = 558 000/m, beta = 15). Density isovalue contours.

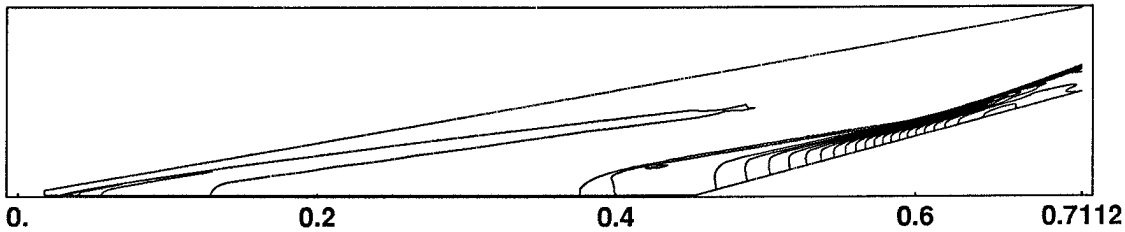

Figure 8. Problem III.4 (Mach = 11.68, Re = 558 000/m, beta = 15).
Pressure coefficient isovalue contours.

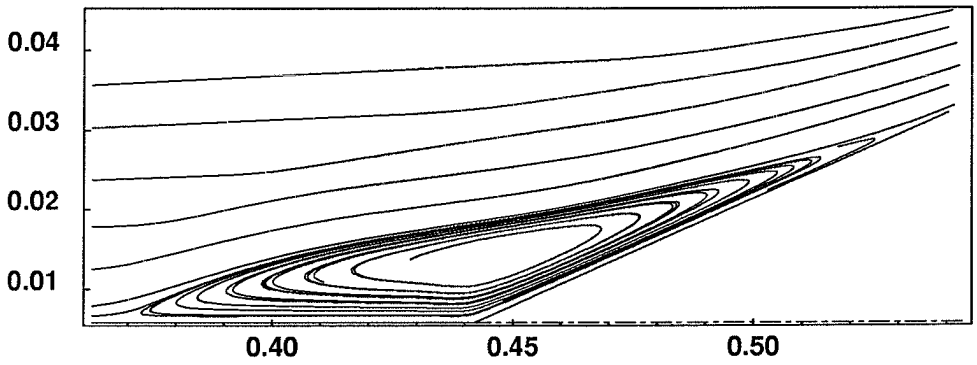

Figure 9. Problem III.4 (Mach = 11.68, Re = 558 000/m, beta = 15).
Detailed view of streamlines.

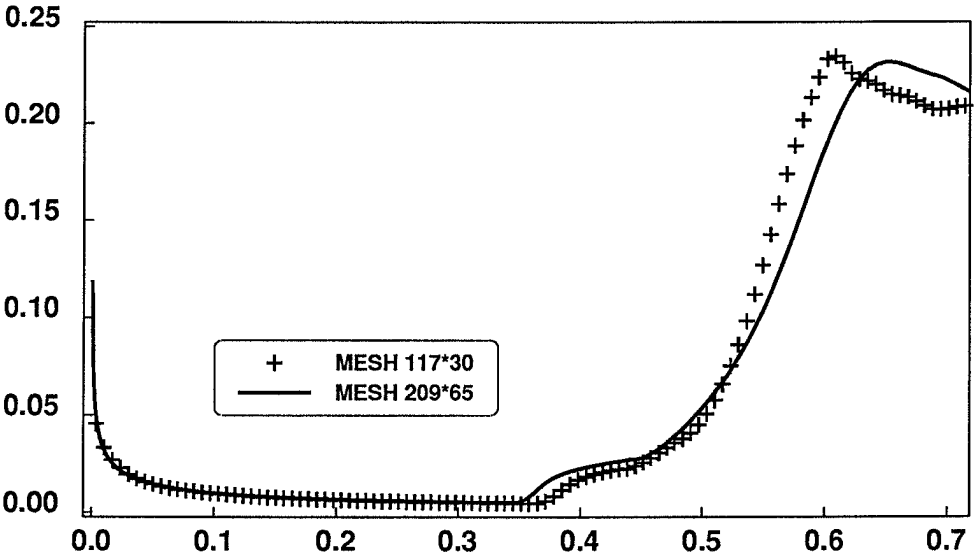

Figure 10. Problem III.4. Pressure coefficient Cp.

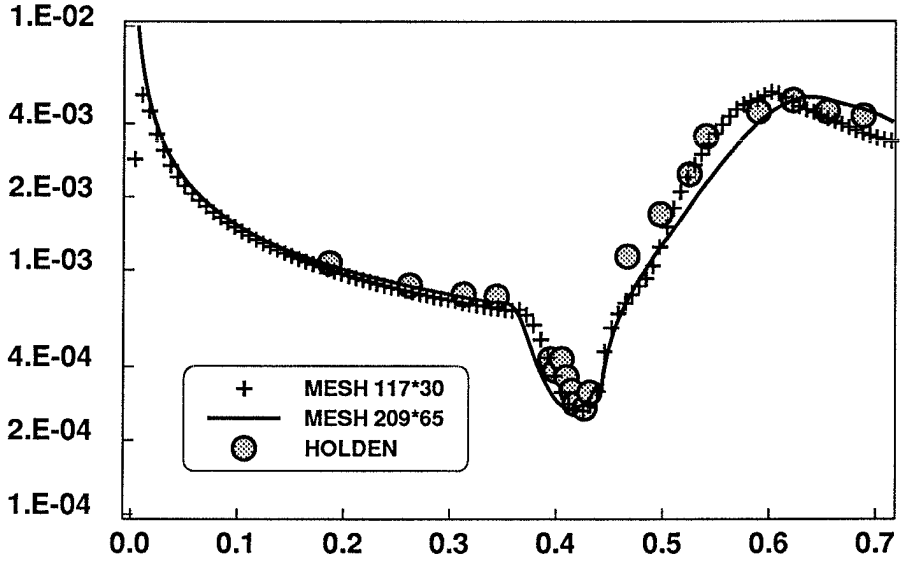

Figure 11. Problem III.4. Stanton coefficient St.

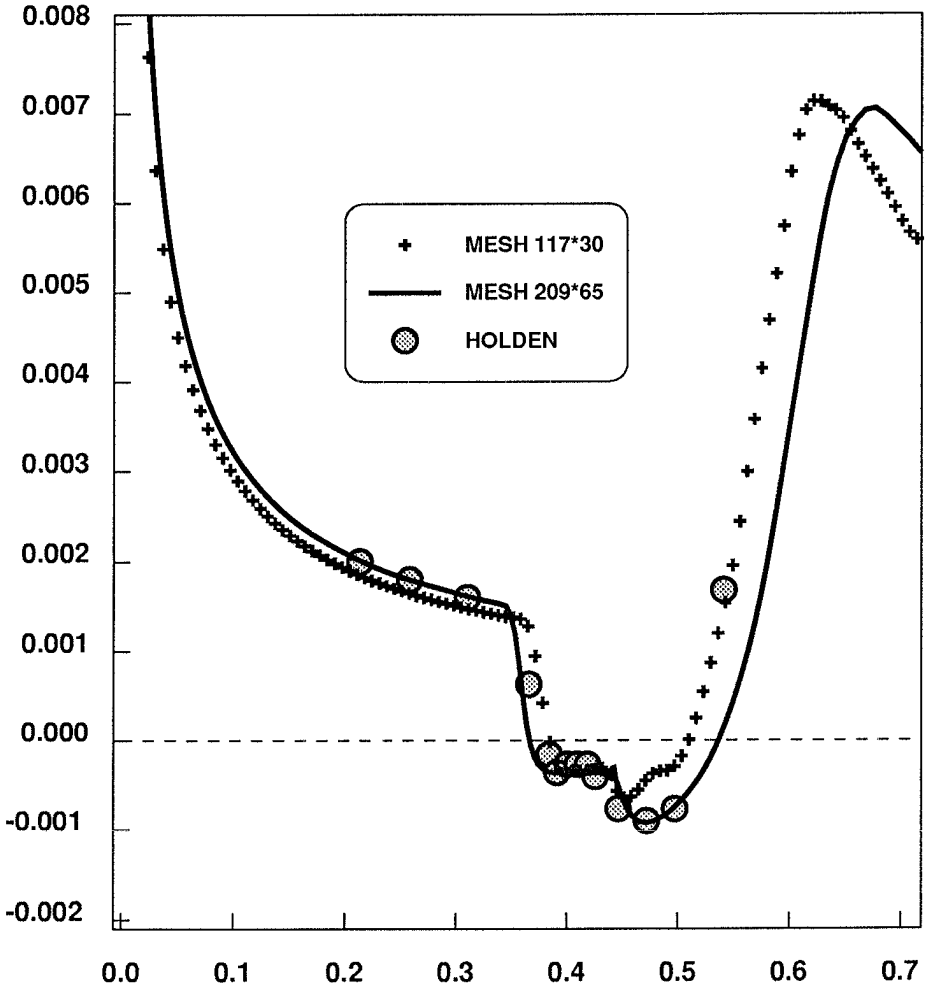

Figure 12. Problem III.4. Skin friction coefficient.